doi:10.1016/j.chroma.2013.07.077

Enhanced Interpretation of Adsorption Data Generated by Liquid Chromatography and by Modern Biosensors

Víctor Agmo Hernandez[2] Jörgen Samuelsson**[1], Patrik Forssén[1], Torgny Fornstedt*[1,2]

[1] Department of Engineering and Chemical Sciences, Karlstad University, SE-651 88 Karlstad, Sweden

[2] Department of Chemistry - BMC, Uppsala University, P.O. Box 579, SE-751 23, Uppsala, Sweden

*Corresponding author information:

Torgny Fornstedt, Professor, Karlstad University, SE-651 88 Karlstad, Sweden

Torgny.Fornstedt@kau.se, +46 76 774 31 58

**Corresponding author information:

Jörgen Samuelsson, PhD, Karlstad University, SE-651 88 Karlstad, Sweden

Jorgen.Samuelsson@kau.se, +46 54 700 1620

Keywords: Chromatography; Biosensors; Surface Plasmon Resonance; Quartz Crystal Microbalance; Data Processing; Fluorescence; Adsorption Isotherm; Adsorption Energy Distribution

Abstract

In this study we demonstrate the importance of proper data processing in adsorption isotherm estimations. This was done by investigating and reprocessing data from five cases on two closely related platforms: liquid chromatography (LC) and biosensors. The previously acquired adsorption data were reevaluated and reprocessed using a three-step numerical procedure: (i) preprocessing of adsorption data, (ii) adsorption data analysis and (iii) final rival model fit. For each case, we will discuss what we really measure and what additional information can be obtained by numerical processing of the data. These cases clearly demonstrate that numerical processing of LC and biosensor data can be used to gain deeper understanding of molecular interactions with adsorption media. This is important because adsorption data, especially from biosensors, is often processed using old and simplified methods.

1 Introduction

It is of increasing importance to adequately measure molecular and bio-molecular interactions since understanding of these interactions is essential in many classic and new research areas such as pharmacology, pharmacokinetics, pharmacodynamics, drug discovery and proteomics. In pharmacokinetics, binding studies are important because only the unbound concentration of the drug is pharmacologically relevant [1]. The unbound concentration of a drug is typically determined by first separating it from the bound fraction with classic techniques such as ultrafiltration or equilibrium dialysis. These time-consuming techniques produce very uncertain results for drugs with high-affinity binding, because of the low resulting unbound concentrations. In drug discovery, rapid determination of drug - target interactions is crucial in a competitive industrial environment and FDA has recently emphasized the need to distinguish enantioselective interactions [2]. Binding studies are also important for potential drug targets and diagnostic markers, including the process to select and optimize lead compounds during drug discovery.

Nonlinear chromatography theory has been extensively developed over the last 30 years and can be used to perform computer simulations [3–8]. The reason for this development is the need to predict/optimize process chromatography and here knowledge about the thermodynamics and kinetics of the system is crucial for successful simulations. High-pressure Liquid Chromatography (LC) instruments have become much more robust and precise over the years and LC therefore serves as a perfect platform for detailed and advanced binding studies. We have recently focused on improving data processing for nonlinear LC. E.g., we have developed an adsorption energy distribution (AED) calculation tool and that has been used, in combination with traditional Scatchard plots, to determine the degree of heterogeneity of the solute-surface interactions without prior assumption of a specific model [6]. Here the adsorption data is processed in a three-step procedure,

(i) Scatchard plots are used to roughly reveal the category of the adsorption: i.e., adsorption of type I, II, III etc. [9].

(ii) AED is calculated to determine the degree of heterogeneity in the interaction: i.e., how many different adsorption sites are present and what is their individual energy of interaction/their abundance (monolayer capacity).

(iii) Model fit: this can be done with only one, or perhaps two, models since the pre-steps have reduced the number of possible models considerably [10–13].

Using modern LC systems and this three-step procedure we have revealed the complicated thermodynamics for several molecular/biomolecular interactions of importance in the life sciences [6,7,12,14,15].

The principles of modern biosensors are very similar to LC because in both platforms we have a surface containing immobilized molecules which is percolated with a solution containing the analyte to be studied. Thus, biosensors can also be used for adsorption studies and for more detailed investigations of the interactions between drug molecules and proteins. We have recently transferred our AED-calculations tools to process data from modern biosensors, such as Surface Plasmon Resonance (SPR) and Quartz Crystal Microbalance (QCM), in order to clarify the molecular interactions between lipoproteins and chondroitin-6-sulfate [14]. From this it is clear that in many cases chromatography models can also be applied to biosensors. The opposite also holds; models developed for biosensors can in many cases be applied to chromatography because similar interactions are studied. In LC we have molecular interactions with an adsorption media and in this sense LC can be regarded as a “sensor”; therefore there are many similarities between the two techniques.

For biosensors based on SPR the studied protein is immobilized on a surface (chip) and then analyte molecules flows over the surface in an analysis cell [10,11]. The binding of analytes to the

immobilized molecules leads to changes of the refractive index at the surface; this in turn causes a shift of the so called SPR-angle which is monitored in real time by an optical sensor. The SPR-signal is proportional to the adsorbed mass and quantification and determination of binding constants can be made. When the adsorbed mass is small, because the analyte molecules to be measured have low molecular weight, the signal-to-noise ratio is low. In recent years, much effort has been made to enhance the optical system to improve the signal-to-noise ratio [16] and to invent new immobilization techniques and chips constructions [17].

QCM is another biosensor technique that can be used to study adsorption phenomena. The technique determines small (in the nano-gram range) changes in the mass loaded onto a sensor. Although originally designed for studying adsorption of rigid materials from a gas phase and the formation of very thin and rigid layers from a liquid [18], the technique has evolved. Nowadays the adsorption of soft viscoelastic material suspended, or dissolved, in a viscoelastic medium can also be studied [19]. This has opened the possibility to study the adsorption of polymer films [19] and of biological material [20–25] as well as to characterize interactions of biological importance [26–31]. In QCM one studies the formation of thin and rigid adsorbed films: the relationship between the measured changes in the quartz crystal oscillation frequency (Δf) and the adsorbed mass (Δm) is given by the Sauerbrey equation [18],

$$\Delta m = -\frac{k}{n}\Delta f\,, \tag{1}$$

where k is a constant depending on the properties of the quartz piece (its fundamental resonance frequency, thickness and density) and n is the overtone number. For a standard quartz crystal with a resonance frequency of 5 MHz, the constant k is 17.7 $ng \cdot cm^{-2} \cdot Hz^{-1}$. Eq. (1) holds even if the crystal is oscillating in a liquid environment. However, certain conditions must be fulfilled: (i) the adsorbed

mass is smaller than the mass of the crystal, (ii) the deposited film is rigid and (iii) the adsorbed material is evenly distributed on the sensor surface.

It is necessary to consider that the QCM response in a liquid environment considers the solvent included in the adsorbed film and can therefore give biased data if the adsorption of heavily solvated compounds is studied. Furthermore, a major drawback of QCM in liquids is that viscous and elastic contributions of the solvent could affect the frequency shift, particularly if the adsorbed material itself forms a viscoelastic film. This is the case for most polymers and proteins, as well as for intrinsically soft structures such as liposomes and lipodisks (planar lipid bilayer structures stabilized by PolyEthyleneGlycol, PEG, modified lipids). Applying Eq. (1) to these systems gives inaccurate results as the loss of energy due to viscoelastic effects is ignored. For the study of these materials by QCM different approaches are employed. Noteworthy are the use of the electromechanical analogy, e.g. see [32], and the use of *ring down* techniques that involves turning off the AC voltage exciting the crystal and measure the decay of the oscillation amplitude. This latter approach is the basis of the QCM with dissipation monitoring technique (QCM-D), which besides the shifts in frequency reports changes in the "dissipation factor" *D*, i.e., a measurement of the energy damping due to the deposited film viscoelasticity. Quantitative determination of the adsorbed mass can be done using the model proposed by Voinova et al. [19] for the formation of viscoelastic films when both the frequency and the dissipation shifts are available at several overtones. In the case of very thin adsorbed films in a bulk liquid, an expression relating the adsorbed mass (Δm), the shift in frequency (Δf) and the shift in dissipation (ΔD) is given by [19,33],

$$\frac{\Delta f}{n} = -\frac{\Delta m}{k} + B\left(n\Delta D\right), \tag{2}$$

where k, n are the same as in Eq. (1) and B is a parameter given by the fundamental oscillation frequency of the crystal and by the viscosity/elastic modulus ratio of the formed film. According to

this equation, a plot of $\Delta f\, n^{-1}$ vs. $n\Delta D$ for different values of n should be a line that intercepts the y-axis at $-\Delta m/k$ and from which the adsorbed mass can easily be calculated [33]. When the thin film assumption does not hold, Eq. (2) cannot be fitted to a line and specialized software such as QTools [34] for QCM-D data analysis is required. QTools can determine both the mass adsorbed and the viscoelastic properties of the film.

For investigations of binding and adsorption behavior in biologically and pharmaceutically important systems there has been a great expansion and refinement of available techniques - such as LC, SPR, QCM, NMR and photo physical techniques [16,17,19,21,22]. Unfortunately, much of the potential information from these improved techniques is lost since the data is often processed and analyzed using simplified methods developed around 50 years ago when the lack of computers made linearization of the data necessary.

The goals of this review are three: (i) to illustrate the transfer of recently developed numerical tools, for processing adsorption data in LC, to a wide variety of different biosensor assays, (ii) to discuss what the signals really tells us and what more detailed information about the interactions can be achieved by data processing and (iii) to compare the two platforms, i.e., nonlinear LC and biosensor technology. We will demonstrate all this be reprocessing and reevaluating data from five previously published studies, two chromatographic cases and three different biosensor assays cases. Case I shows how the evaluation procedure can be used to gain deeper understanding of chromatographic interactions. Case II shows how adsorption data, in this case generated by LC perturbation experiments, can be further processed for deeper understanding of retention and adsorption mechanisms. For this case the same interactions was studied using SPR and the two techniques are compared. In case III, Quartz Crystal Microbalance (QCM) is used to characterize the adsorption behavior of phosphorylated peptides on titanium dioxide using a rigid film approach. In case IV QCM

sensors modified with viscoelastic films is used for peptide-lipodisk interaction studies. Finally, in case V the same interactions as in case IV are studied, but by using a fluorimetric approach instead.

2 Theory

Here we will present the relevant theory that applies both to LC and to biosensors.

2.1 Adsorption Isotherms

An adsorption isotherm describes the relationship between adsorbed (q) and free concentration (C) of the solute at a constant and specific temperature [3]. In this section we are going to briefly discuss the different models used in this study.

Adsorption isotherms can be determined using several experimental methods. However, in the end, they will all give a signal that is proportional to the adsorbed amount (q) of solute, but in some cases the measured response need to be preprocessed.

One of the simplest adsorption models, where the solute is reversibly adsorbed at a limited number of identical adsorption sites, is the Langmuir adsorption isotherm. To handle heterogeneous adsorption one can expand the simple Langmuir model to the *n*-Langmuir adsorption isotherm model by assuming n independent adsorption sites, the equation is then,

$$q = \sum_{i=1}^{n} \frac{K_i q_{s,i} C}{1 + K_i C}, \tag{3}$$

where K_i and $q_{s,i}$ are the association equilibrium constant and the monolayer saturation capacity for the i:th site, respectively. Observe that for n = 1 we have the Langmuir model and if n = 2 we have the bi-Langmuir model. The initial slope of the adsorption isotherm gives the sum of the distribution coefficients for all sites which is equivalent to the sum of the products $q_s \cdot K$ for all sites.

In this study one system was previously described using a two layer BET adsorption isotherm [26]. However, in this study the Moreau model is used instead because: (i) the Moreau and the two layer BET are mathematically identical and (ii) in a previous paper [32] we investigated how to calculate the AED using Moreau model. The Moreau model is,

$$q = q_s \frac{KC + hK^2C^2}{1 + 2KC + hK^2C^2}, \quad (4)$$

where K is the association equilibrium constant and h is the adsorbate - adsorbate interaction intensity constant. If $h = 0$ the Moreau model is almost identical to the Langmuir model and only if $h \neq 0$ can the adsorption isotherm contain physically realistic inflection points.

2.2 AED

In most cases a heterogeneous adsorption process is described using adsorption isotherms, e.g. Tóth, bi-Langmuir etc. Another way is to extend the adsorption isotherm to a continuous distribution of independent homogeneous sites across a certain range of adsorption energies ($d\ln K$),

$$q(C) = \int_{K_{min}}^{K_{max}} f(\ln K) \cdot \theta(K, C) \cdot d\ln K dK, \quad (5a)$$

$$\theta(K, C) = \frac{KC}{1 + KC}, \quad (5b)$$

$$\theta(K, C) = \frac{KC + hK^2C^2}{1 + 2KC + hK^2C^2}, \quad (5c)$$

$f(\ln K)$ is the adsorption energy distribution where K has an exponential relationship with adsorption energy according to the Arrhenius equation and $\theta(K, C)$ is the local adsorption isotherm model. As local adsorption models mainly the Langmuir model, Eq. (5b), has been used. But for concave adsorption isotherm, and adsorption isotherms with inflection points, the BET [35] and the Moreau [36], Eq. (5c), model can be used. The main difference when calculating the AED using the Moreau

model, compared to the Langmuir model, is that one has to set *h* (a similar constant exist in the BET model). The solutions will depend on the selection of *h* [36], however the number of adsorption sites seems to be conserved as long as the *h*-value used in the AED calculation is not much higher than the "true" *h*-value [36]. The AED is solved using the expectation maximization method, where the integral equation is solved in an iterative manner [37,38].

2.3 Processing Adsorption Data

There are many pitfalls when determining binding data, i.e., adsorption isotherm determination. E.g. we need sufficient number of data points spread over a sufficient broad concentration range. But even if these criteria are fulfilled it is necessary to properly process the adsorption data and not wasting it using a simple linearized approach to derive the binding constants, e.g. by only using Scatchard plots [39].

In this study we will use a three step-procedure to analyze and process the adsorption data. First, Scatchard plots (q/C vs q) are used, not to determine adsorption isotherm parameters but to determine possible adsorption isotherm models that can be used to describe the data. Scatchard points are extremely useful for identifying the type of the adsorption isotherm, e.g. Type I convex, Type III concave or Type II, which can be described as a combined Type I and III with an inflection point in between. The simplest convex isotherm is the Langmuir model which describes the interaction with a single adsorption site. The Tóth and the bi-Langmuir models are simple heterogeneous Type I adsorption isotherms; the difference being that the Tóth model have heterogeneous interactions on a single site whereas the bi-Langmuir model have two isolated different adsorption sites. It is impossible/hard to distinguish between these two heterogeneous models by fitting directly to adsorption data. But by using the combined approach with Scatchard plots and AED-calculations it is possible as illustrated in Fig. 1 where dataset 1 - 3 describes Langmuir, Tóth and Bi-Langmuir adsorption, respectively. An inspection of the Scatchard plots in Fig. 1a shows

that the Scatchard plot is linear for dataset 1 and but not for dataset 2 and 3. Linear Scatchard plots are only possible for the Langmuir model but concave Scatchard plots are possible for both the Tóth and the bi-Langmuir model. Since the Tóth model describes an adsorption where only one type of interaction exist, but the bi-Langmuir model have two distinct adsorption sites with different adsorption energy, distinguishing between the two heterogeneous models is mechanistically very interesting. However, traditional tools for model fitting cannot distinguish between the adsorption models. But if we also do AED calculations (Fig. 1b), we can see that dataset 1 and 2 have a unimodal AED and dataset 3 have a bimodal AED. With the combined information, we can conclude that dataset 1 most probably can be described using the Langmuir model, dataset 2 can be described with an adsorption model with an unimodal heterogeneous AED, e.g. the Tóth model, and dataset 3 can be described with an adsorption model with a bimodal AED, e.g. the bi-Langmuir model. Using the two first steps in our three step procedure, i.e., Scatchard plots and AED-calculations, we can, by understanding the binding mechanism, considerably reduce the number of possible adsorption models prior to the third step: nonlinear model fitting.

3 Cases

The aim of this study is to process adsorption and binding data generated by LC and by biosensors, with some emphasis on the latter. We will focus on what the signal really tells us and the deeper understanding we achieve using the numerical three-step data processing approach: (i) Scatchard plots, (ii) AED-calculations and (iii) rival model selection.

In case I, we exemplify the conclusions that can be drawn from the data processing described above for a nonlinear LC system. The same conclusions would be impossible to arrive at using the traditional procedure of fitting rival models to experimental data followed by statistical evaluation.

In case II a detailed investigation is made of the β-blocker propranolol binding to immobilized Cel7a cellulose. We will process adsorption data from the LC perturbation method using a SPR based Biacore 2000 assay as reference, in [12] this was investigated at different buffer pH and here the LC data is processed further. Case II illustrates a common case where the adsorption is clearly heterogeneous which is easily detected using the three-step adsorption data processing.

In case III, QCM is used to characterize the adsorption behavior of phosphorylated peptides on titanium dioxide [26]. One of the studied peptides showed a clear deviation in adsorption behavior and the corresponding adsorption data was processed further in this study. The studied peptide was of special interest since it shows structural similarities with most peptides expected from the enzymatic digestion of a biological sample. This case illustrates how to handle adsorption data that are described with a more complex adsorption isotherm and we will show how Scatchard plots can be used to reveal inflection points.

In case IV, QCM sensors modified with immobilized soft viscoelastic films are used to study peptide - lipodisk interactions. More specifically, we studied lipodisks for the peptide mastoparan (wasp poison) and mastoparan X, where the peptide sequence has been modified to become fluorescence [40]. The association isotherms obtained utilizing QCM were re-evaluated by the three-step data processing procedure. This case illustrates two aspects: (i) the importance of preprocessing the adsorption data prior the adsorption analysis and (ii) fluorescent modification of the peptide will strongly affect the determined adsorption isotherm parameters.

In case V, the same peptide interaction as in case IV is investigated by using the fluorimetric approach. This is possible since the spectrum of free tryptophan-containing peptide in water is red shifted compared to when it is associated to the lipid membrane. This shift can be used to determine the proportion of bound and free peptide, thus providing the data to construct an association isotherm that describes the peptide - lipodisk affinity. Even if the method has the drawback that it

cannot be used with peptides with no tryptophan residues it is an interesting opportunity to compare two completely different biosensor principles such as QCM and fluorimetry. This case is illustrates the same interactions as in case IV but now with the peptide in free solution and not immobilized on a surface. This approach will lead to data with no immobilization effects but other challenges need to be handled.

3.1 CASE I: Nonlinear LC

Here we use the procedure described above, and shown in Fig. 1, for a nonlinear LC system. We investigated the retention mechanism for the separation of glycine dipeptide (GG) and tripeptide (GGG) on 12% cross-linked agarose gel media, using mobile phases consisting of varying contents of acetonitrile in water [8]. The peptides retention times increased with increasing acetonitrile content in the eluent, demonstrating that polar binding prevails in this phase system and GGG had larger retention than GG because the larger possibilities for hydrogen bonds in case of the larger peptide.

A nonlinear adsorption study was undertaken at different acetonitrile content in the eluent, using the elution by characteristic points (ECP) method on strongly overloaded peptide peaks. The combined analysis of the Scatchard plots and the AED-calculations was done when the acetonitrile content in the eluent was varied from 0 to 20%. The interactions started out being homogenous (GG), or mildly heterogeneous (GGG). When the acetonitrile content increased a more or less stronger degree of heterogeneity around one site was observed. Finally, when the acetonitrile content increased further a typical bimodal energy interaction consisting of two sites was observed (GGG at 10 and 20 %). In Fig. 2b, it can be seen how the AED of GG at 0% acetonitrile has a narrow homogenous interaction (Fig. 2a, black line) and when the acetonitrile content in the eluent increases the AED successively becomes more heterogeneous (Fig. 2a, dashed and grey lines). In the case of GGG the interactions becomes bi-modal at the highest acetonitrile contents (cf. Fig. 2b).

The Tóth and bi-Langmuir models described these interesting adsorption trends excellently [8]. The distinction between the two of heterogeneity models, Tóth and bi-Langmuir, is important in order to understand if we have a mixed mode electrostatic/hydrogen bonding, that can be described by bi-Langmuir, or only hydrogen bonding, that in this case can be described by the Tóth model. If one only has hydrogen bonding the heterogeneity is caused by hydrogen bonds at different positions, i.e., there is in only one site (unimodal interactions) that have different energy levels (Fig. 2a, dashed and grey lines and Fig. 2b, black line in). Without the data processing it would have been impossible to distinguish between the principally different Tóth and bi-Langmuir models since the data fits somewhat better to bi-Langmuir from a statistically point of view.

3.2 CASE II: SPR and Enantioselective LC

Here we will study the binding of the β-blocker propranolol enantiomers to Cel7a cellulose, at pH 4.5 and 7.5, [12] using the LC perturbation method and the focus will be on reprocessing the nonlinear adsorption data [3,41]. At the time the study was performed the AED-tool was not available and these calculations are performed here instead in order to gain more knowledge.

The same enantioselective drug protein interactions have also been studied using a SPR-based Biacore 2000 biosensor assay. In [41,42] the authors clearly showed that using LC it is possible to measure the individual enantiomer adsorption isotherms by analyzing the racemic mixture. This is not possible using SPR as only the total adsorption is measured and consequently the enantiomers must be analyzed separately, however, the required amounts of protein and drug are much smaller for SPR because of the miniaturized format. Also notice that two component LC data cannot be used for AED calculations because the tool is currently not able to handle these complicated data sets. Another advantage of LC is that it is possible to determine the amount of protein in the column, e.g. by using by amino acid analysis. This is not possible using SPR because of the small amounts immobilized protein on the chips. In a recent similar study it was concluded that nonlinear LC is best

suited for weaker interactions and SPR for stronger interactions. In fact it is impossible to achieve information about very strong molecular interactions using chromatography [13].

In Fig. 3 the LC perturbation result for R- and S-Propranolol on immobilized Cel7a is presented [12]; each enantiomer was injected in a series of 24 concentration levels ranging from 1.0 μM to 2.0 mM, i.e., a two thousand fold range. The Scatchard plot (Fig. 3, middle row) are curved indicating heterogeneous interactions according to the discussion in section 2.3. Moreover, the Scatchard plot contains two asymptotes, one associated with the low and the other with the high concentration range. This pattern is characteristic for a two site model, e.g. the bi-Langmuir model, with large energy difference between the two adsorption sites. The AED-calculations (Fig. 3, bottom row) for both pH-values and both enantiomers are at least bimodal. The AED-plots shows interesting differences in the adsorption at pH 4.5 and 7.5. The difference in energy of interaction (ln *K*) between the two adsorption sites is larger at the high pH, in other words the degree of heterogeneity is larger at pH 7.5 than at pH 4.5. The combined AED calculations and Scatchard plots indicate that the bi-Langmuir model could be used to describe the adsorption data well and that when pH is increased both the affinity and the enantio-selectivity of the interaction are increased. The bi-Langmuir models fitted to the experimental data are presented as curves in Fig. 3, top and middle row.

The combined Scatchard plots and AED-calculations approach revealed both the degree of heterogeneity and its pH dependence. If we only had used low concentration data only the first asymptote would have been observed (*cf*. Fig. 3 middle row) [5]. This would lead to the wrong conclusion that a more homogeneous adsorption model, e.g. the Langmuir model, describes the data well. This clearly illustrates the importance of a using a wide concentration range for adsorption measurements, especially for the Scatchard plots.

3.3 CASE III: QCM - Rigid Films

In a recent study by Eriksson et al. [26] QCM and Eq. (1) were used to determine the adsorption isotherms of phosphorylated peptides on titanium dioxide (TiO_2). As a uniform and rigid layer of adsorbed material is expected, the Sauerbrey relationship should hold. The phosphopeptide-TiO_2 system is of great importance, given that although TiO_2 is widely used with several techniques for phosphopeptide enrichment prior to analysis, the adsorption of phosphorylated peptides on TiO_2 had not been systematically characterized. The cited report pinpointed some of the main parameters defining the peptides affinity for the surface (amino acid sequence, degree of phosphorylation and salt content of the solution) and identified possible sources for biased results in most enrichment protocols. Furthermore, it was demonstrated that most of the studied peptides, with a high degree of confidence, followed the Langmuir adsorption isotherm. However, one of the studied peptides, IR (a tri-phosphorylated peptide derived from the insulin receptor), showed positive cooperativity and clearly deviated from ideal behavior. This particular peptide is of special interest since it has structural similarities with most peptides expected from the enzymatic digestion of a biological sample, i.e., peptides with a positive charged amino acid at one end.

The adsorption of the IR peptide could be best described by a two layer liquid-solid extended BET isotherm [43] that considers different association constants for the peptide - TiO_2 and the peptide - peptide interactions. By determining the association parameters at different salt concentrations, it was established that the peptide - peptide interaction was mainly of electrostatic origin.

Fig. 4 shows the obtained isotherms and the corresponding Scatchard plots comparing the adsorption behavior of the IR peptide on TiO_2 QCM sensors when no salt was added and when 50 mM $NaClO_4$ was included in the bulk solution. The concentration of the IR peptide ranged from 0.01 µM to 10 µM. To illustrate the use of AED for this system a Moreau isotherm was fitted to the data. Although the physical meaning the two layers BET and Moreau adsorption isotherm Eq. (4) differ,

346 they both represent likely scenarios and both fit the data well. The latter is preferred in this report,
347 as the AED calculations have not been adapted to use two layer BET adsorption isotherms; see
348 section 2.2. The AED calculations support the conclusion reported in the original manuscript
349 concerning the electrostatic nature of the interactions. The calculated adsorption parameters are
350 shown in Table 1. According to the Moreau model the conclusion is that the peptide - peptide
351 interaction is strong and increases with the ionic force. The first statement agrees with the
352 conclusions reached by Eriksson et al., while the second contradicts them. This is an example of when
353 two models provide reasonable results but lead to different conclusions. In complex systems, such as
354 the one described, it is likely that the real adsorption behavior has characteristics of both the BET
355 and the Moreau models.

356 To conclude, the QCM experiments performed by Eriksson et al in [26] proved to be a powerful tool
357 for systematic characterization of peptide - TiO_2 interactions. Together with the three steps analysis
358 method presented here, the obtained data is a source of very useful information that provides
359 several alternative interpretations to better understand the adsorption process.

360 ### 3.4 CASE IV: QCM - Viscoelastic Films

361 Here we analyzed recently reported data [33] concerning the immobilization of lipodisks and their
362 association with alpha-helical amphiphilic peptides. These peptides have enormous potential for
363 pharmaceutical applications, as they may show antimicrobial activity. Incorporation of these
364 peptides into lipodisks allows a sustained release of the compound and, at the same time, the
365 peptide is protected from enzymatic degradation [44]. In the cited study it was very important to
366 accurately determine the amount of material (lipodisks in this case) that is bound on the surface.
367 Given that lipodisks are not rigid structures, using the Sauerbrey approach, Eq. (1), would give
368 inaccurate results. In the cited study, it was determined, using the Voinova approach, Eq. (2), that full
369 coverage of the sensor surface with lipodisks was achieved when 2600 $ng \cdot cm^{-2}$ of the material had

been immobilized. If the Sauerbrey approach had been used instead, several problems would have arisen. First, each overtone would provide with a different answer and second, these answers would most likely significantly underestimate the real adsorbed amount. In the study we refer to, the amount of material immobilized would then have been 1770 ng·cm^{-2} for the 3:rd overtone and 900 ng·cm^{-2} for the 11:th overtone.

The cited paper studied and reported the association isotherms of three different peptides (melittin, mastoparan, and mastoparan X) with the lipodisks. Fig. 5 show a reevaluation of the reported data for mastoparan (MAS) and mastoparan X (MAS-X) according to the procedure described in the Theory section. The figure shows the difference in the interpretation of the data when the viscoelastic properties of the material are accounted for by the Voinova approach and when the Sauerbrey approach is used. Furthermore, the analysis of the data sheds some light on the nature of the peptide-lipodisk interaction. The original report established that the association data could be described both by a bi-Langmuir isotherm and by an isotherm proposed by Pérez-Paya et al. which accounts for peptide - peptide interactions as well as for changes in the lipodisk structure upon peptide binding [45]. As for the IR peptide example described in the previous section, the most likely explanation is that the real association behavior shares characteristics with both models.

In the report discussed here, direct fitting of the data to a bi-Langmuir adsorption isotherm provided trivial parameters. Therefore, the authors reported only “apparent” association data using the Langmuir isotherm. Fig. 5 show that the data treatment described in the Theory section enables fitting the data to the bi-Langmuir model and thus extracting useful information. The results are summarized in Table 2 and can be interpreted in the light of previous knowledge concerning the lipodisk-peptide interactions [46]. It is known that amphiphilic peptides have a high affinity for the lipodisk edges, while their affinity for the planar faces is much lower. The interactions with the two bi-Langmuir sites can therefore be assumed to represent the lipodisk edges (high affinity for the

peptides) and the lipodisk flat faces (lower affinity). The data in Table 2 agrees with this interpretation as a small number of high affinity sites (described by $R_{eff(max)1}$ and K_1) are found together with a larger number of low affinity sites ($R_{eff(max)2}$ and K_2); here the former represent the lipodisk edges and the latter the planar faces of the disks. Although the model provides a reasonable interpretation of the data, it is necessary to consider that the Pérez-Paya model fits the data well and is related to a plausible physical interpretation. As stated above, the most likely scenario is that the association behavior has, at least, both a bi-Langmuir component (two kinds of adsorption sites) and a Pérez-Paya component (peptide-peptide interactions and modification of the lipodisk properties upon peptide binding). Both models can be used to predict the association behavior, but it is necessary to consider that, separately, they provide only partial physical interpretations of the association phenomena.

3.5 CASE V: Fluorimetric Determinations

Peptide binding to lipodisks can also be determined using fluorimetric methods when a tryptophan residue is found in the peptide. The emission spectrum of this amino acid is dependent on the polarity of its surroundings. The spectrum of a free tryptophan-containing peptide in water is red shifted compared to when it is associated with the lipid membrane. This shift can be used to determine the proportions of bound and free peptide, thus providing the data to construct an association isotherm that describes the peptide-lipodisk affinity. Experimentally a solution of the studied peptide is titrated with small additions from a lipodisks dispersion, this means that the association isotherm is constructed starting from the high concentration end. The fluorimetric approach has the advantage of providing a much larger number of experimental points in a single measurement. However, the method's drawback is that it cannot be used with peptides with no tryptophan residues. As suggested recently [29], artificially labeling the peptide may drastically change the association behavior, and should therefore be avoided. Furthermore, the possible effects

418 of starting at high peptide to lipid ratios need to be considered. Finally, the association behavior at
419 low bulk peptide concentrations is not available, and, therefore, important information concerning
420 the interaction with the high affinity sites is lost.

421 Fig. 6 shows the association isotherm of MAS-X (reported in [33]) obtained with the fluorimetric
422 method. As in the case of the QCM-D determinations, the authors [33] concluded that the data fitted
423 very well to both the Pérez-Paya model and to the bi-Langmuir model, although, for the latter only
424 trivial results could be obtained. Fig. 6 shows that, with help of the data processing proposed in the
425 Theory section, the bi-Langmuir association parameters can be estimated and are: $R_{eff(max)1}$ = 0.068; K_1
426 = 2.55 μM^{-1}, $R_{eff(max)2}$ = 0.043 and K_2 = 0.21 μM^{-1}. The order of magnitude of the affinity constants
427 corresponds well with what is obtained with the QCM-D, see previous section. The $R_{eff(max)}$ values,
428 however, do not correspond to the assumption that the low affinity interaction represent association
429 with the planar part of the disks. This discrepancy is probably due to the following three facts: first,
430 (i) the component of the isotherm described by the Pérez-Paya model is not considered; see the
431 previous section. Then, (ii) the association data at low peptide bulk concentrations is not available
432 and, therefore, important information concerning the high energy interaction could be missed.
433 Finally, (iii) fluorimetric determinations, that start the collection of data at very large peptide to lipid
434 ratios, may cause significant structural changes in the lipodisks. Among these structural changes, the
435 dissolution of the disks into micelle-like structures cannot be discarded [47,48] These structures
436 present a high curvature, similar to the lipodisk edges, and therefore have a high affinity for the
437 peptides, as demonstrated previously [46]. They may therefore provide the extra number of
438 calculated high affinity binding sites. These structural changes are minimized with the QCM-D
439 approach, where low peptides to lipid ratios are measured first. Furthermore, if structural changes
440 occur, they are reflected in the QCM-D response, as shown recently [33]. In the fluorimetric
441 experiments, on the other hand, no information about the structure is available, and it is therefore
442 unknown what kind of structures that are actually being studied in the high bulk peptide

concentration range. The parameters calculated here, however, support the hypothesis of high curvature aggregates being formed at high peptide concentrations.

4 Conclusions

By reprocessing previously acquired data from LC and three principally different biosensor assays we have demonstrated the importance of proper data handling throughout the whole process: from the determination of possible adsorption isotherms to the final model fitting. We can divide this process into three steps: (i) preprocessing of adsorption data, (ii) adsorption data analysis and (iii) final rival model fit. The second step prior to the model fit is to analyze the data by combining Scatchard plots with AED calculations (*cf.* Fig. 1) and this will significantly reduce the number of possible adsorption models.

In case I, we illustrated how this three-step processing of LC adsorption data can be used to distinguish between two mechanistically totally different heterogeneous models: one with mixed electrostatic/hydrogen bonds and one with hydrogen bonds with different energies. These two models would have been impossible to distinguish otherwise.

In case II, data from LC perturbation experiments were further treated numerically with the suggested three-step procedure [12]. In this case the heterogeneous adsorption was clearly shown using the combined Scatchard and AED-calculation approach, a classic linearization using only Scatchard plots would have missed this. This case also shows the importance of having a large concentration range because the Scatchard plot contains two asymptotes, one associated with the low and the other with the high concentration range. Without the high concentration range data one could easily have mistaken the adsorption process for a homogeneous Langmuir model.

In case III QCM was used to characterize the adsorption behavior of phosphorylated peptides on TiO_2. The adsorption data in this case where described with an adsorption isotherm containing an

inflection point and we demonstrated how this was easily observed in the Scatchard plot. This case also shows that the adsorption processing approach used in this study is capable of handling even complicated adsorption models that contains inflection points, such as the Moreau model.

In case IV interaction between the peptide mastoparan and mastoparan X with lipodisks were investigated using QCM-D and this case highlights two important issues. First, the importance of preprocessing the measured data to make sure that the data used is proportional to adsorbed amount. The second issue was that even small changes in the peptide sequence can lead to large differences in the adsorption properties. For both peptides, it was possible to reveal that the association behavior probably has, at least, both bi-Langmuir and Pérez-Paya adsorption components. Therefore these models can, separately, only provide partial physical interpretations of the association phenomena.

One drawback with measuring adsorption isotherms using LC, QCM and SPR is that the ligand is immobilized on a surface and this is probably also going to affect the measured adsorption isotherm. One solution to this is to measure the interaction in free solution by using a fluorescence assay as we did in the case V for mastoparan X. Here we noted that the order of magnitude of the affinity constants corresponds well with the ones obtained in case IV, but the assumption that the low affinity interaction represents association with the planar part of the disks, as was concluded in case IV does not hold. This discrepancy could be due to several reasons, e.g. that fluorimetric determination may cause significant structural changes in the lipodisks. These structural changes are minimized with the QCM-D approach and if they occur it is reflected in the QCM-D response, but not in the fluorimetric experiments. This therefore demonstrates that the measurement itself could modify the studied system.

The above clearly demonstrates that much more information can be extracted from the adsorption data using the three steps adsorption data processing approach compared to the classical

linearization and use of the Langmuir model. Moreover, the data processing tools developed are not platform dependent and can be used for both LC and biosensors.

Acknowledgements

We are thankful to Anna Eriksson (Department of Chemistry-BMC, Uppsala University) for providing complementary data concerning the IR isotherms. We also thank Prof. Katarina Edwards, Department of Chemistry-BMC, Uppsala University, for fruitful discussions and for providing resources and facilities. This work was partially supported by the Swedish Research Council (VR) for the project "Fundamental Studies on Molecular Interactions Aimed at Preparative Separations and Biospecific Measurements" (grant 621-2012-3978).

References

[1] J. Gabrielsson, D. Weiner, Pharmacokinetic and Pharmacodynamic Data Analysis: Concepts and Applications, Fourth Edition, 4th ed., Swedish Pharmaceutical Press, 2007.

[2] Chirality 4 (1992) 338.

[3] G. Guiochon, D.G. Shirazi, A. Felinger, A.M. Katti, Fundamentals of Preparative and Nonlinear Chromatography, 2nd ed., Academic Press, Boston, MA, 2006.

[4] A. Seidel-Morgenstern, J. Chromatogr. A 1037 (2004) 255.

[5] J. Samuelsson, R. Arnell, T. Fornstedt, J. Sep. Sci. 32 (2009) 1491.

[6] J. Samuelsson, A. Franz, B.J. Stanley, T. Fornstedt, J. Chromatogr. A 1163 (2007) 177.

[7] G. Götmar, J. Samuelsson, A. Karlsson, T. Fornstedt, J. Chromatogr. A 1156 (2007) 3.

[8] X. Zhang, J. Samuelsson, J.-C. Janson, C. Wang, Z. Su, M. Gu, T. Fornstedt, J. Chromatogr. A 1217 (2010) 1916.

[9] S.J. Gregg, K.S.W. Sing, Adsorption, Surface Area, and Porosity, Academic Press, London, 1982.

[10] R. Karlsson, J. Mol. Recognit. 17 (2004) 151.

513 [11] R.L. Rich, Y.S.N. Day, T.A. Morton, D.G. Myszka, Anal. Biochem. 296 (2001) 197.
514 [12] R. Arnell, N. Ferraz, T. Fornstedt, Anal. Chem. 78 (2006) 1682.
515 [13] P. Sandblad, R. Arnell, J. Samuelsson, T. Fornstedt, Anal. Chem. 81 (2009) 3551.
516 [14] K. Lipponen, P.W. Stege, G. Cilpa, J. Samuelsson, T. Fornstedt, M.-L. Riekkola, Anal. Chem. 83
517 (2011) 6040.
518 [15] T. Fornstedt, J. Chromatogr. A 1217 (2010) 792.
519 [16] I. Maier, M.R.A. Morgan, W. Lindner, F. Pittner, Anal. Chem. 80 (2008) 2694.
520 [17] O.R. Bolduc, J.-F. Masson, Anal. Chem. 83 (2011) 8057.
521 [18] G. Sauerbrey, Z. Phys. 155 (1959) 206.
522 [19] M.V. Voinova, M. Rodahl, M. Jonson, B. Kasemo, Phys. Scr. 59 (1999) 391.
523 [20] B. Reiss, A. Janshoff, C. Steinem, J. Seebach, J. Wegener, Langmuir 19 (2003) 1816.
524 [21] C. Fredriksson, S. Khilman, B. Kasemo, D.M. Steel, J. Mater. Sci. Mater. Med. 9 (1998) 785.
525 [22] M. Rodahl, F. Höök, C. Fredriksson, C.A. Keller, A. Krozer, P. Brzezinski, M. Voinova, B. Kasemo,
526 Faraday Discuss. 107 (1997) 229.
527 [23] J. Wegener, J. Seebach, A. Janshoff, H.-J. Galla, Biophys. J. 78 (2000) 2821.
528 [24] J. Wegener, A. Janshoff, C. Steinem, Cell Biochem. Biophys. 34 (2001) 121.
529 [25] J. Wegener, A. Janshoff, H.-J. Galla, Eur. Biophys. J. 28 (1998) 26.
530 [26] A.I.K. Eriksson, K. Edwards, A. Hagfeldt, V.A. Hernández, J. Phys. Chem. B 117 (2013) 2019.
531 [27] G. McCubbin, S. Praporski, S. Piantavigna, D. Knappe, R. Hoffmann, J. Bowie, F. Separovic, L.
532 Martin, Eur. Biophys. J. 40 (2011) 437.
533 [28] S.J. Fraser, X. Mulet, L. Martin, S. Praporski, A. Mechler, P.G. Hartley, A. Polyzos, F. Separovic,
534 Langmuir 28 (2011) 620.
535 [29] E. Meiby, M. Morin Zetterberg, S. Ohlson, V. Agmo Hernández, K. Edwards, Anal. Bioanal. Chem.
536 405 (2013) 4859.

[30] K. Vainikka, K. Reijmar, G. Yohannes, J. Samuelsson, K. Edwards, M. Jussila, M.-L. Riekkola, Anal. Biochem. 414 (2011) 117.

[31] V. Agmo Hernandez, K. Reijmar, K. Edwards, Anal. Chem. (2013) 130705083926004.

[32] V. Agmo Hernández, J. Niessen, F. Harnisch, S. Block, A. Greinacher, H.K. Kroemer, C.A. Helm, F. Scholz, Bioelectrochemistry 74 (2008) 210.

[33] V. Agmo Hernández, K. Reijmar, K. Edwards, Anal. Chem. Submitted (n.d.) Submitted.

[34] QCM-D Data Analysis, available at: http://www.q-sense.com/data-analysis-2.

[35] F. Gritti, G. Guiochon, J. Colloid Interface Sci. 264 (2003) 43.

[36] M. Enmark, J. Samuelsson, T. Undin, T. Fornstedt, J. Chromatogr. A 1218 (2011) 6688.

[37] B.J. Stanley, G. Guiochon, Langmuir 10 (1994) 4278.

[38] B.J. Stanley, G. Guiochon, J. Phys. Chem. 97 (1993) 8098.

[39] H. Xuan, D.S. Hage, Anal. Biochem. 346 (2005) 300.

[40] C.L. Longland, M. Mezna, F. Michelangeli, J. Biol. Chem. 274 (1999) 14799.

[41] J. Lindholm, P. Forssén, T. Fornstedt, Anal. Chem. 76 (2004) 5472.

[42] P. Forssén, J. Lindholm, T. Fornstedt, J. Chromatogr. A 991 (2003) 31.

[43] F. Gritti, W. Piatkowski, G. Guiochon, J. Chromatogr. A 978 (2002) 81.

[44] M.M. Zetterberg, K. Reijmar, M. Pränting, Å. Engström, D.I. Andersson, K. Edwards, J. Controlled Release 156 (2011) 323.

[45] E. Pérez-Payá, I. Porcar, C.M. Gómez, J. Pedrós, A. Campos, C. Abad, Biopolymers 42 (1997) 169.

[46] A. Lundquist, P. Wessman, A.R. Rennie, K. Edwards, Biochim. Biophys. Acta-Biomembr. 1778 (2008) 2210.

[47] P. Wessman, M. Morin, K. Reijmar, K. Edwards, J. Colloid Interface Sci. 346 (2010) 127.

[48] A.A. Strömstedt, P. Wessman, L. Ringstad, K. Edwards, M. Malmsten, J. Colloid Interface Sci. 311 (2007) 59.

FIGURE CAPTIONS

Figure 1: Illustration of (a) the Scatchard plot and (b) the corresponding AED calculations for three different adsorption data sets. Dataset 1 is a Langmuir adsorption model, dataset 2 a Tóth adsorption model and dataset 3 a bi-Langmuir adsorption model.

Figure 2: AED-calculations for (a) GG and (b) GGG at different eluent contents of acetonitrile: 0% (black solid lines), 10% (dashed lines) and 20% (gray solid lines). The AED were calculate using 300 grid points and 200 000 iterations. Reprinted from Ref. [8], Copyright 2013, with permission from Elsevier.

Figure 3: Association isotherms (top), Scatchard plots (middle), and AED calculations (bottom) using 300 grid points and 100 000 iterations describing the adsorption of R-propranolol (left) and S-propranolol (right) on Cel7a. Calculated from experimental data reported by Robert Arnell et al. [12], symbols are experimental data, lines are fitted data and Ru is response units.

Figure 4: Adsorption isotherms (top left), Scatchard plots (top right) and AED calculations using 300 grid points, 100 000 iterations and a *h*-value of 200 (bottom) describing the adsorption of IR on TiO_2 QCM sensors. Black line: with no added salt, gray line: with 50 mM NaClO4 added. Experimental data are from [26].

Figure 5: Association isotherms (top), scatchard plots (middle) and AED calculations using 300 grid points and 100 000 iterations (bottom) for mastoparan (left) and mastoparan X (right), respectively. Calculated from experimental data reported by Agmo Hernández et al [33], R_{eff} is effective associated peptide/lipid mole ratio.

Figure 6: Association isotherm (top left), scatchard plot (top right) and AED calculated using 300 grid points and 500 000 iterations (bottom) for mastoparan X. Calculated from fluorimetric data reported by Agmo Hernández et al [33].

Table 1: Adsorption parameters of IR on TiO2 according to the Moreau isotherm

$NaClO_4$ [mM]	*K* [μM^{-1}]	*h*
0	0.566	235
50	0.063	2631

Table 2: Peptide-lipodisk association parameters according to the bi-Langmuir isotherm and comparison between the results obtained when considering the lipodisk film as rigid (Sauerbrey model) and when considering the viscoelasticity of the structure (Voinova).

Peptide	Model	$R_{eff(max)1}$	K_1 [μM^{-1}]	$R_{eff(max)2}$	K_2 [μM^{-1}]
Mastoparan	Sauerbrey	0.1	138	0.30	1.60
	Voinova	0.085	186	0.28	1.94
Mastoparan X	Sauerbrey	0.084	4.5	699	3.37×10^{-6}
	Voinova	0.043	16.8	0.07	0.32

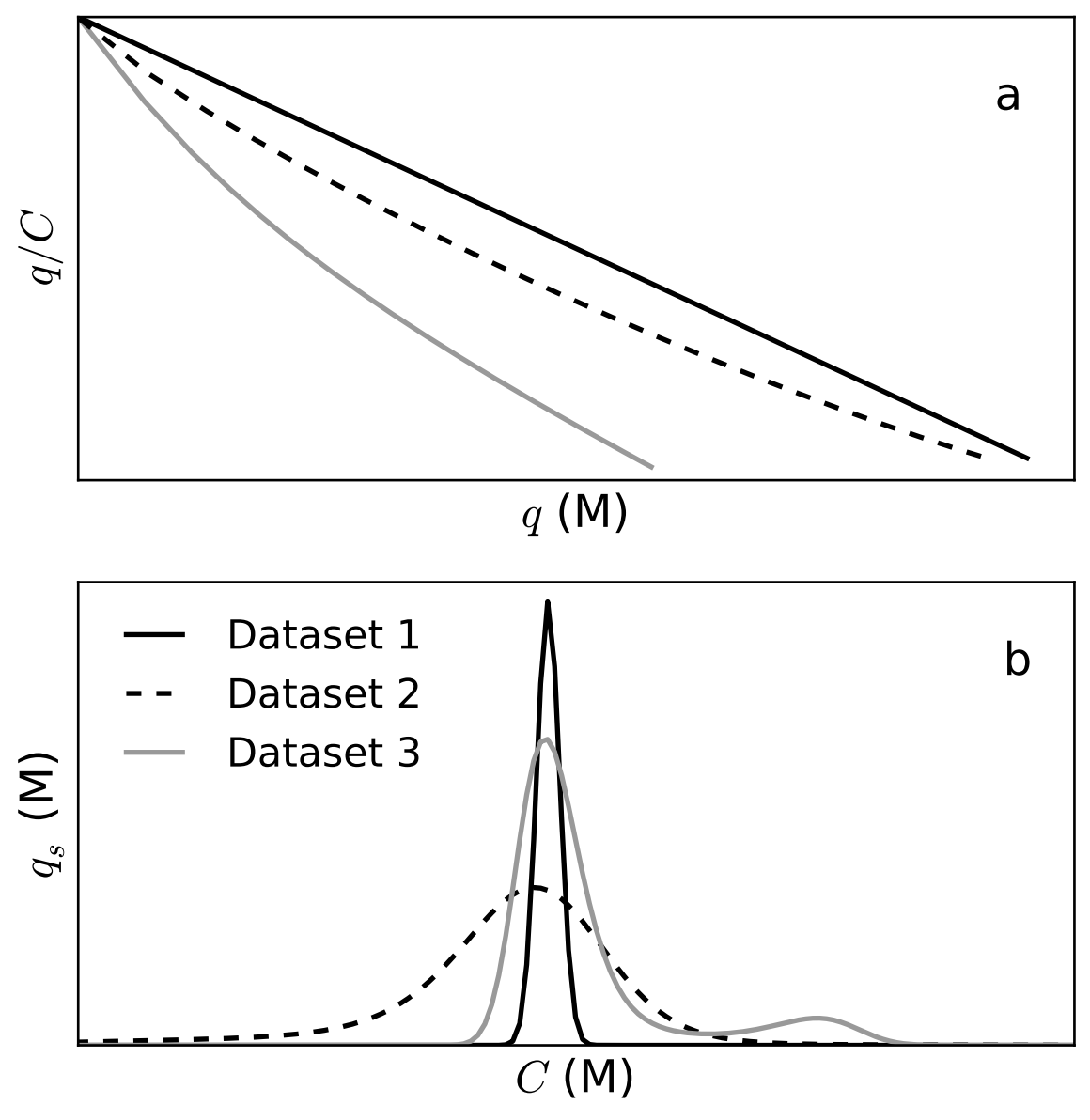
a
q/C
q (M)
b
Dataset 1
Dataset 2
Dataset 3
q_s (M)
C (M)

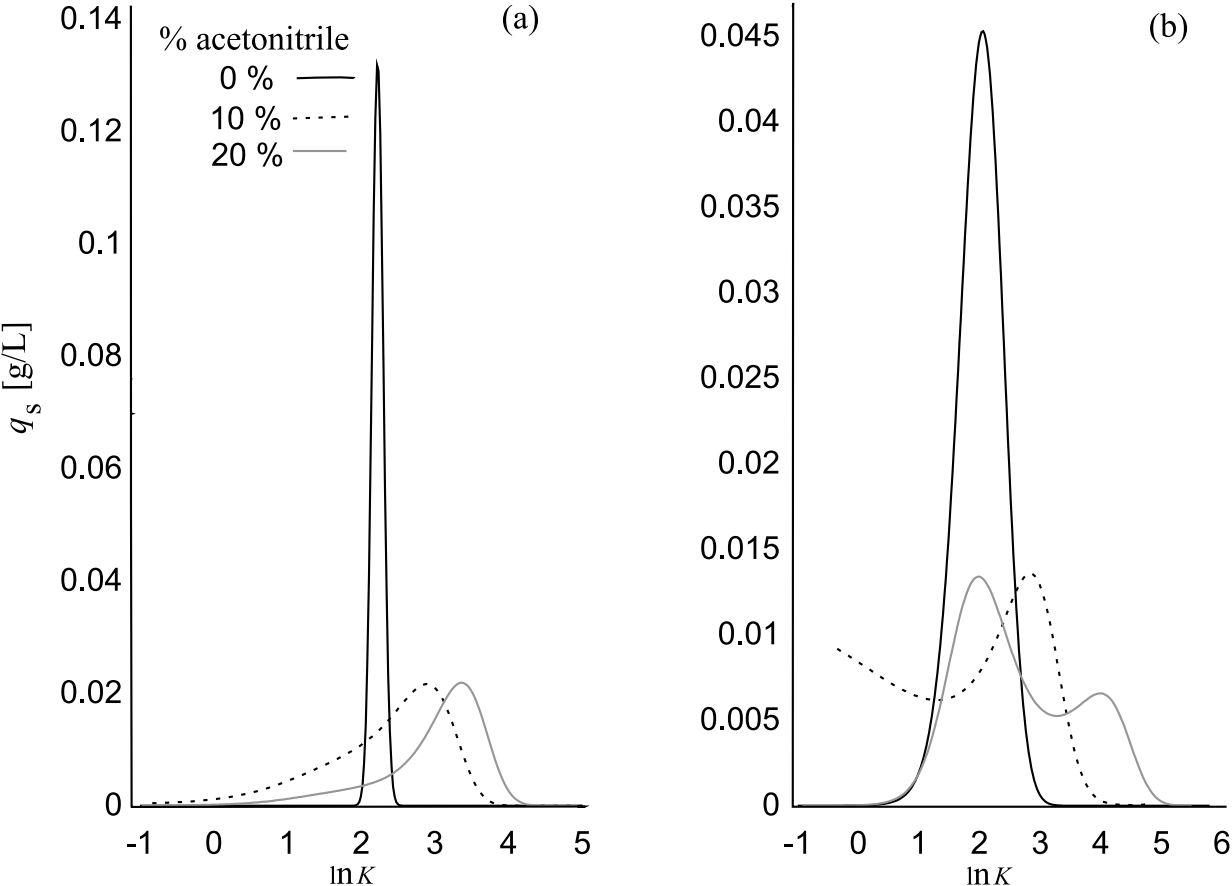
(a)
% acetonitrile
0 %
10 %
20 %
q_s [g/L]
0.14
0.12
0.1
0.08
0.06
0.04
0.02
0
-1
0
1
2
3
4
5
ln K
(b)
0.045
0.04
0.035
0.03
0.025
0.02
0.015
0.01
0.005
0
-1
0
1
2
3
4
5
6
ln K

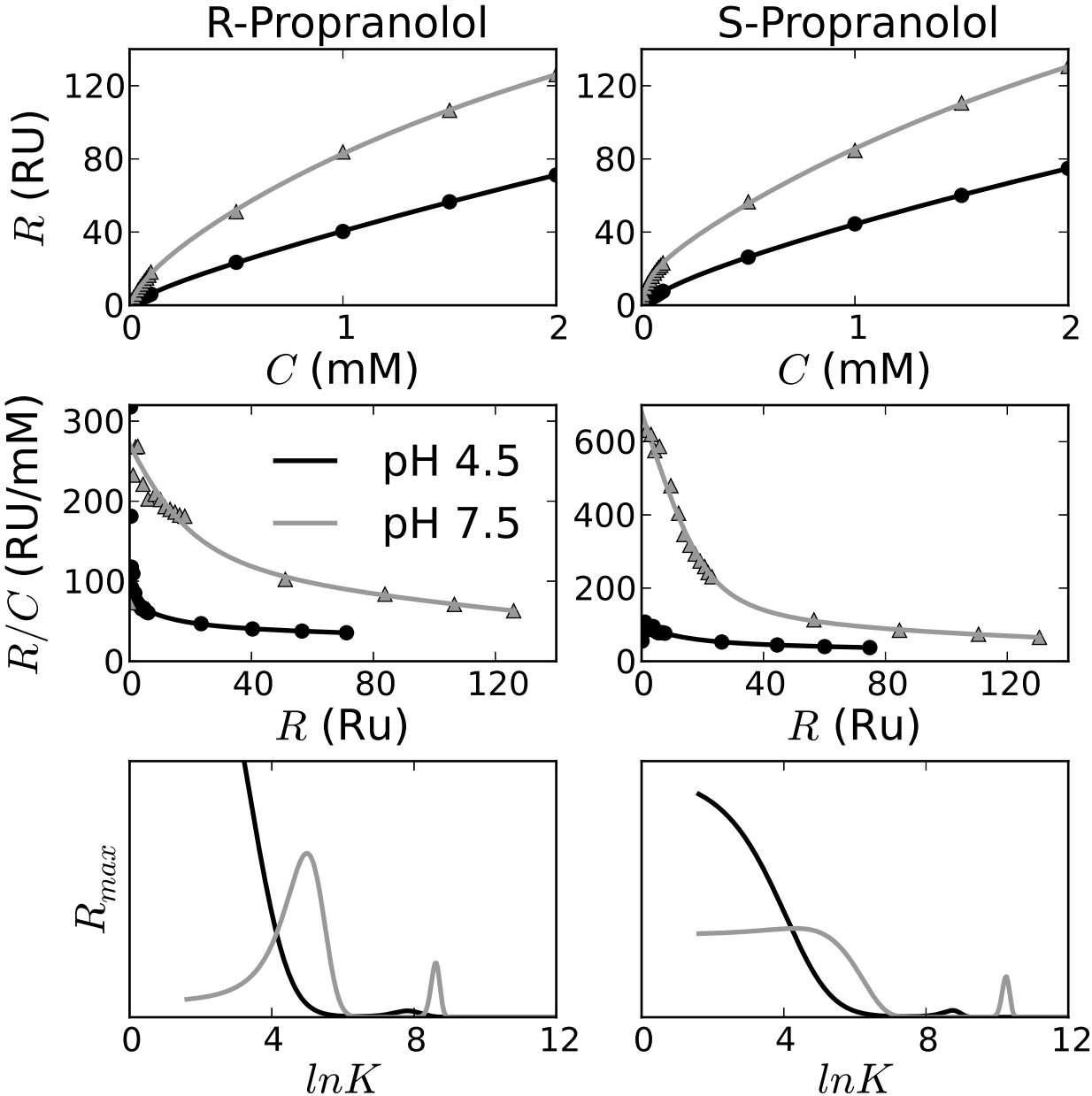
R-Propranolol
S-Propranolol
R (RU)
C (mM)
R/C (RU/mM)
R (Ru)
pH 4.5
pH 7.5
R_max
lnK

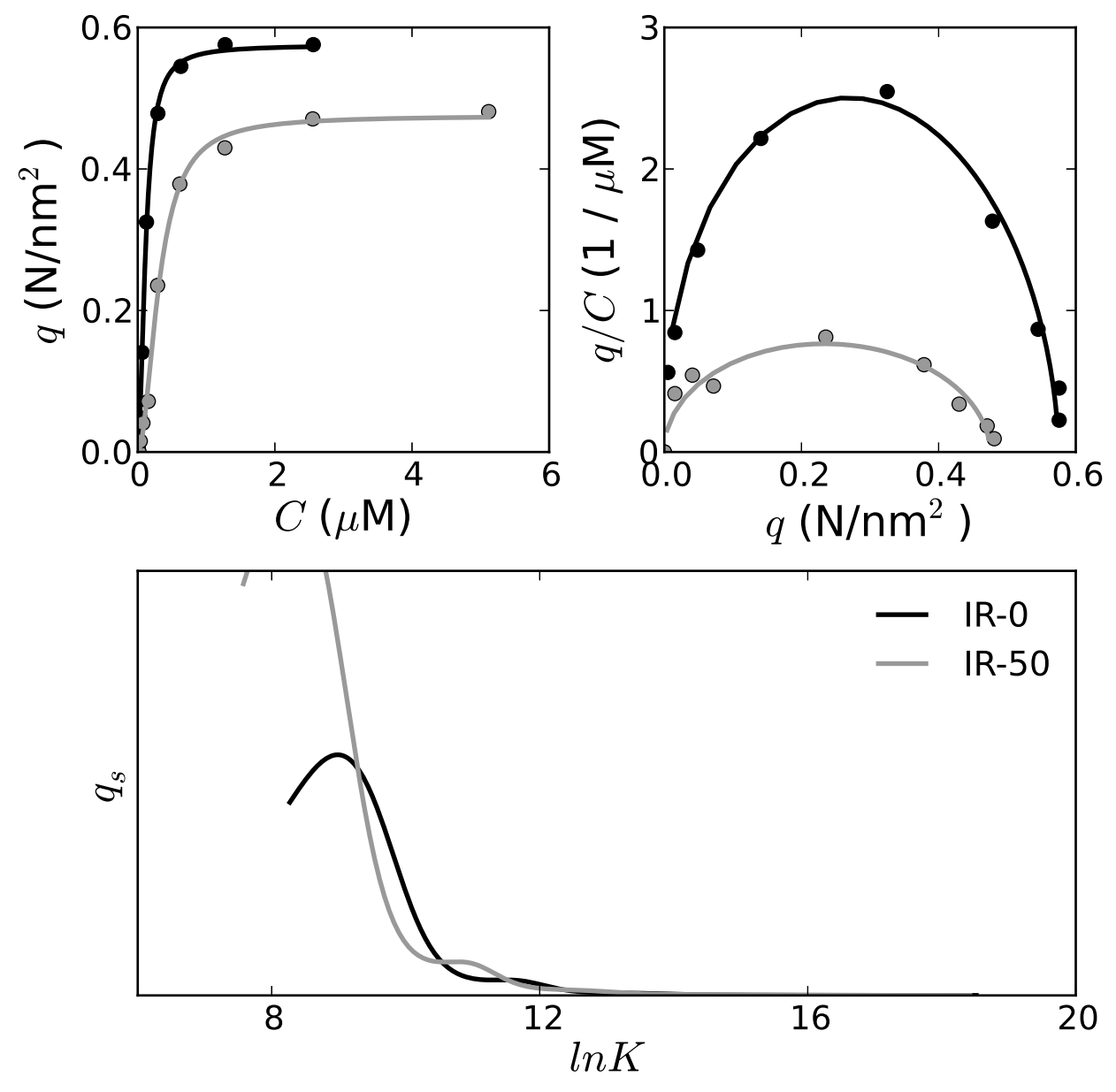
0.6
0.4
0.2
0.0
q (N/nm^2)
0
2
4
6
C (μM)
3
2
1
0
q/C (1 / μM)
0.0
0.2
0.4
0.6
q (N/nm^2)
IR-0
IR-50
q_s
8
12
16
20
lnK

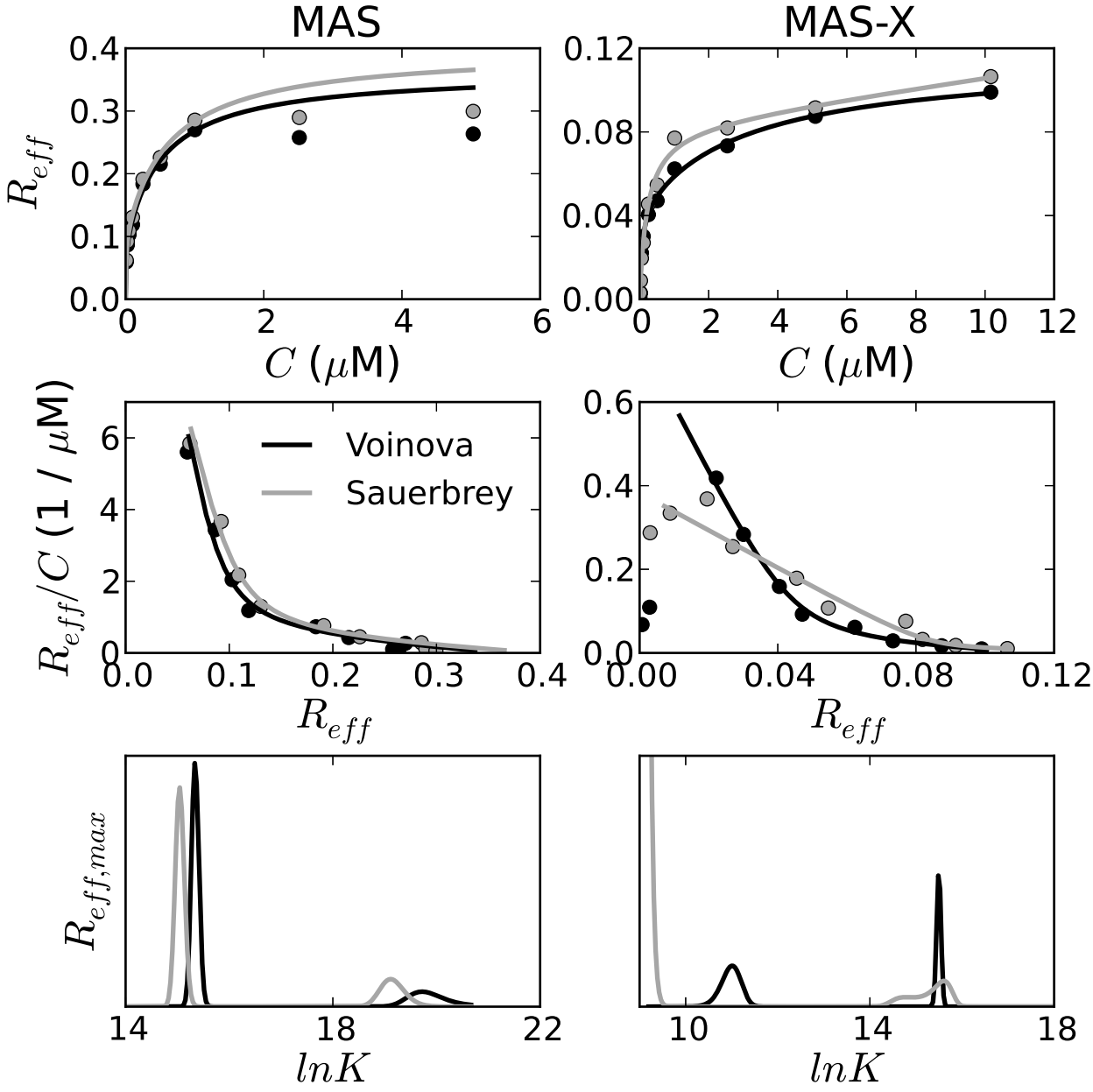
MAS
MAS-X
R_{eff}
C (μM)
R_{eff}/C (1 / μM)
Voinova
Sauerbrey
$R_{eff,max}$
lnK

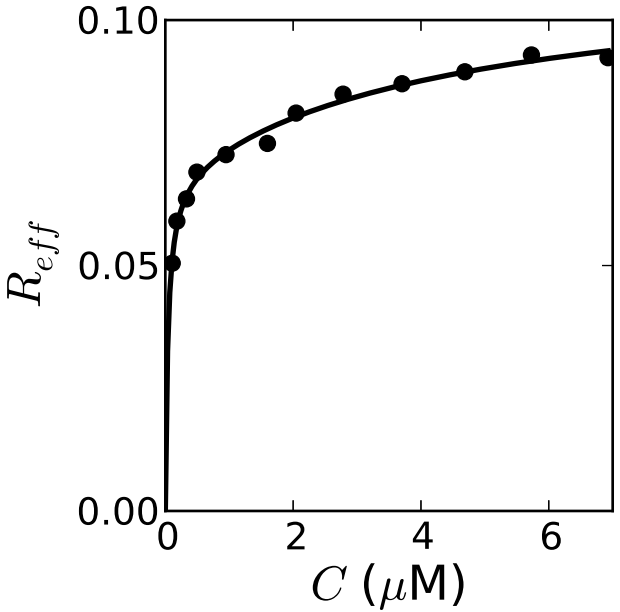
0.10
0.05
0.00
0
2
4
6
R_{eff}
C (μM)

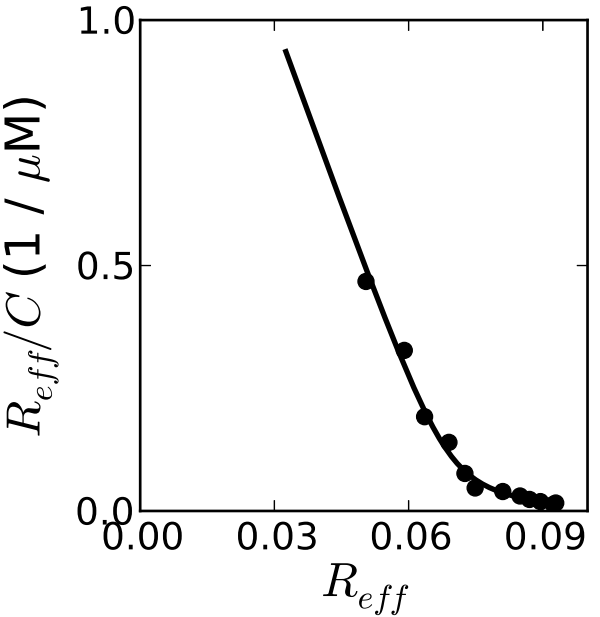
1.0
0.5
0.0
0.00
0.03
0.06
0.09
R_{eff}/C (1 / μM)
R_{eff}

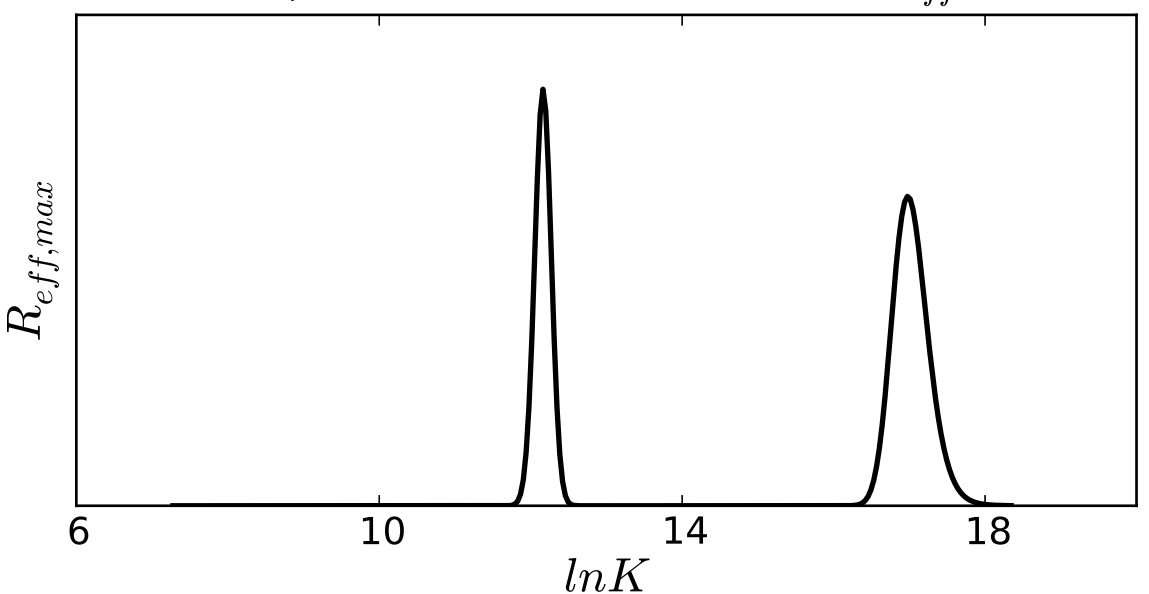
6
10
14
18
$R_{eff,max}$
lnK